

Research



Cite this article: Kitavtsev G, Münch A, Wagner B. 2018 Thin-film models for an active gel. *Proc. R. Soc. A* **474**: 20170828. <http://dx.doi.org/10.1098/rspa.2018.0828>

Received: 1 December 2017

Accepted: 21 November 2018

Subject Areas:

applied mathematics, mathematical modelling, biophysics

Keywords:

liquid crystals, asymptotic analysis, active matter

Author for correspondence:

B. Wagner

e-mail: wagnerb@wias-berlin.de

Thin-film models for an active gel

G. Kitavtsev¹, A. Münch¹ and B. Wagner²

¹Mathematical Institute, University of Oxford, Andrew Wiles Building, Oxford OX2 6GG, UK

²Weierstraß Institute, Mohrenstrasse 39, 10117 Berlin, Germany

BW, 0000-0001-8306-3645

In this study, we present a free-boundary problem for an active liquid crystal starting with the Beris–Edwards theory that uses a tensorial order parameter and includes active contributions to the stress tensor and then derive from it the Eriksen model for an active polar gel and scalar order parameter to analyse the rich defect structure observed in applications such as the adenosinetriphosphate-driven motion of a thin film of an actin filament network. The small aspect ratio of the film geometry allows for an asymptotic approximation of the free-boundary problem in the limit of weak elasticity of the network and strong active terms. The new thin-film model captures the defect dynamics in the bulk as well as wall defects and thus presents a significant extension of previous models based on the Leslie–Erickson–Parodi theory. As an example we derive the explicit solution for an active gel confined to a channel, which has discontinuous director profile leading to a bidirectional flow structure generated by the active terms.

1. Introduction

Since the works by Simha & Ramaswamy [1] and Kruse *et al.* [2] active liquid crystals have been used extensively as a hydrodynamic theory to describe the ordered motion of large numbers of self-propelled particles, such as bacterial suspensions, fibroblast monolayers or the adenosinetriphosphate (ATP)-driven actin network that underlies the movement of the lamellopodium of a crawling cell. The different levels of description, from the microscopic to the continuum hydrodynamic theory of this rapidly expanding research field has been reviewed in Marchetti *et al.* [3].

In many studies, active matter extensions are based on the Leslie–Eriksen–Parodi (LEP) theory [4–6] such as in [7,8], where active polar gels were derived from thermodynamic principles. The model in [7]

and the simplified version in [9] are augmented by sources of energy due to ATP hydrolysis that drives the system and makes the bulk of the cell an *active* (polar) gel. The bulk liquid i.e. the gel is characterized mainly by the velocity and the director field, which describes the averaged orientation of the actin filaments at a given point in space and time. The driving force is provided in their models via the chemical potential difference of ATP and its hydrolysis products. This hydrolysis of ATP fuels the molecular motors to generate forces along the actin network, and is also used for the polymerization and depolymerization of the network filaments.

As in passive liquid crystals, defects are a common phenomenon and their dynamics is strongly influenced by the fact that the system is out-of-equilibrium due to the energy source from the active terms. Observations in *in vitro* experiments [10] show that they may directly depend on strength of the activity, where it was demonstrated that the observed defects tend to disappear again for sufficiently high levels of activity [11]. Based on the LEP theory, point defects such as asters, vortices and spirals were described [2,7]. Furthermore, phase diagrams of unbounded two-dimensional states [9] as well as flow transitions in confined films [12] were investigated. In particular, it was found that spontaneous flow arises in a confined active polar gel (with no-slip or free-slip conditions at the domain walls) above a critical layer thickness. This transition was also described within a thin-film model with a free, capillary surface [13].

However, there are some inherent deficiencies to describe local defect structures basing on the LEP theory, which is connected to the discontinuity of the director field and the infinite associated local elastic energy at the defect points. This problem becomes even more critical for the description of wall and line defects along which the elastic energy in the LEP theory is essentially discontinuous and, in particular, standard energy renormalization techniques cannot be applied. Moreover, when modelling the evolution of thin nematic films with moving contact lines using LEP theory, related problems occur due to singularity of the director field at the contact line [14–21]. Therefore, more general approaches such as the Beris–Edwards theory [22,23] of liquid crystal hydrodynamics, that use a tensorial order parameter, the so-called Q -tensor, instead of a director field, have been devised. Extensions of this theory by active terms go back to Marenduzzo *et al.* [24,25] and have been extended in two and three dimensions to various problems involving different geometries, such as spherical shells [26,27], and have been investigated in a number of directions [28–33]. But even for the passive Beris–Edwards theory, the conditions at boundaries and in particular, stress and anchoring conditions at free interfaces are less well studied within this model. Important contributions to these issues can be found in [17,34,35]. In particular, it was conjectured [36] that a Q -tensor-based approach might facilitate the resolution of nematic point defects in the vicinity of moving film contact lines [37]. On the other hand, most biologically active gels form polar (rather than nematic) liquid crystalline order, the fact which encourages for derivation of an intermediate model, which, on one hand, operates with polar director field and, on the other, is capable for smooth resolution of the observed defect structures. A good candidate for such model is provided by the Ericksen model first suggested in [38].

The derivation of the corresponding thin-film model is the goal of this article. We begin by formulating the active Beris–Edwards model (§2) including all the boundary conditions for a two-dimensional cross section of a thin film. We emphasize that basic features of the two-dimensional Beris–Edwards model resemble those of its three-dimensional version, but that it also has independent interesting two-dimensional applications in biology [29,39], also on curved surfaces for thin shells of active matter [26,27]. In this case, we are able to represent the Q -tensor through a scalar order parameter q and the director field n and reduce the active Beris–Edwards model to the corresponding active Ericksen model [38] that describes the coupled evolution of q and n . Making use of the scale separation of the thin-film geometry, a leading-order approximation is derived (§3) in the limit of weak elasticity and strong active terms to arrive at a new thin-film model, both for the passive and active cases. We also show that our model formally reduces to the one based on LEP theory, when the scalar order parameter q is homogeneous, and coincides with one of [17] in the passive case.

Finally, in §4, we derive explicit solutions for special cases of flat constant films and small angle mismatch between the anchoring conditions. They show that in the passive case solutions with

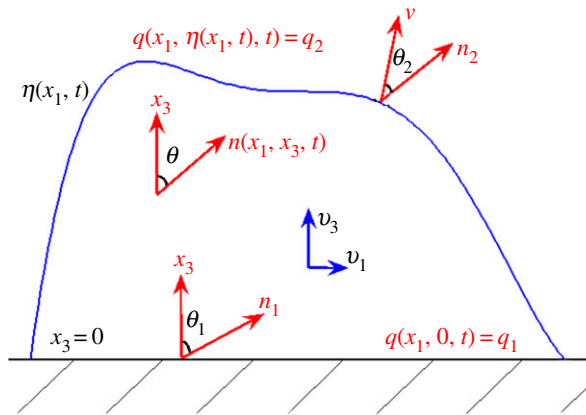


Figure 1. Sketch of the geometry of a thin film together with variables involved in the Q -tensor system (2.4)–(2.6). (Online version in colour.)

nonlinear nematic fields exist when certain compatibility relations between film thickness and nematic boundary conditions are satisfied. In particular, in paragraph 4.2 we construct solutions with the director field being discontinuous across the special isotropic line along which $q = 0$ (figure 2*a,b*). These solutions can be viewed as the limiting profiles as the elastic constant tends to zero of the antisymmetric nematic field in the channel observed numerically in [40], cf. in particular with the approximate formula (29) therein, see also [41]. In the presence of active terms, some of the found passive solutions continue to exist and exhibit non-zero flow that can be spontaneously initiated from zero, for example, by increasing the film thickness, similar to the effect observed in [9,12]. In particular, the solution with initially discontinuous director profile initiates a counter-flow (figure 2*c*) in the presence of small active terms with fluid moving into opposite directions (prescribed by the director field) in the lower and upper half of the film.

A discussion of further extensions and applications concludes the paper (§5). In appendix A, we present the rescaled Ericksen model under the thin-film approximation. In appendix B, we derive the polar thin-film model based on the LEP system with active terms.

2. Formulations of active liquid crystal models

(a) Beris–Edwards model for an active gel

Instead of treating the active gel through a theory based on the LEP formulation for liquid crystals [4–6], we include the corresponding terms into the Beris–Edwards theory that uses Q -tensors to describe liquid crystals and is a popular field of research across the theoretical literature [23,42–45], see also the recent overviews [46,47], as a more general alternative theory for liquid crystals. In a subsequent step, we express the two-dimensional Q -tensor in terms of the director field and an additional scalar order parameter to obtain an Ericksen-type model introduced in [38], for which we then derive the thin-film model in §3. An active gel model in terms of Q -tensors and its subsequent reformulation is also given in [25], but we additionally need to include appropriate conditions at the free interface, which we base on [34,48].

We only consider two-dimensional models here and introduce a spatial domain Ω with coordinates (x_1, x_3) , while t represents time, (see figure 1 for a schematic sketch of the geometry and variables involved). The Beris–Edwards model is associated with the standard Landau–de Gennes energy in the form [49]

$$\mathcal{F}_{LG}[Q; \Omega] = \int_{\Omega} (f_e(Q) + f_b(Q)) dx, \quad (2.1)$$

where $Q \in H^1(\Omega, \mathcal{L}_0)$ takes on values in the space of the symmetric and traceless matrices, or Q -tensors,

$$\mathcal{L}_0 := \{Q \in \mathbb{R}^{2 \times 2}, Q = Q^T, \text{tr}(Q) = 0\}.$$

In (2.1), the bulk contribution is given by

$$f_b(Q) = -\frac{a^2}{2} \text{tr}(Q^2) + \frac{c^2}{4} (\text{tr}(Q^2))^2, \quad (2.2)$$

with constants a, c and

$$f_e(Q) = \frac{L_1}{2} Q_{ij,k} Q_{ij,k} \quad (2.3)$$

is the elastic contribution, with an elastic constant $L_1 > 0$. (We deliberately avoid further complications by considering a model with only one elastic constant.) Here, and elsewhere (except in appendix A), we use the usual convention that duplicate indices are summed over and indices with commas indicate spatial derivatives, e.g. $Q_{ij,k}$ is used for the derivative of Q_{ij} with respect to x_k for $i, j, k = 1, 2, 3$.

In the most general form, the active Beris–Edwards model can be written as (see [23,27,43,44] and references therein)

$$0 = \partial_i v_i, \quad (2.4)$$

$$0 = -\partial_i p + \mu \partial_i^2 v_i + \partial_j (\tau_{ij} + \sigma_{ij} - \zeta \Delta \chi Q_{ij}) \quad (2.5)$$

$$Q_t + (v \cdot \nabla) Q = \Gamma H + S(\nabla v, Q) + \lambda_1 \Delta \chi Q, \quad (2.6)$$

where v_i and p are the velocity components and the pressure, μ the isotropic viscosity and Γ a collective rotational diffusion constant. The term

$$S_{ij} = (\xi e_{ik} + \omega_{ik}) \left(Q_{kj} + \frac{\delta_{kj}}{2} \right) + \left(Q_{ik} + \frac{\delta_{ik}}{2} \right) (\xi e_{kj} - \omega_{kj}) - 2\xi \left(Q_{ij} + \frac{\delta_{ij}}{2} \right) (Q_{mk} u_{k,m}), \quad (2.7)$$

with

$$e_{ij} = \frac{1}{2} (\partial_j v_i + \partial_i v_j), \quad \omega_{ij} = \frac{1}{2} (\partial_j v_i - \partial_i v_j), \quad I_{ij} = \delta_{ij}, \quad (2.8)$$

describes how the flow gradient rotates and stretches the order-parameter. The scalar parameter $\xi \in \mathbb{R}$ appearing both in equations (2.5) and (2.6) depends on the molecular details of a given liquid crystal. The active terms are associated with the activity parameters ζ and λ_1 and have been introduced in (2.5) and (2.6) as in [25,27]. As in [25], we have an active term in the linear momentum equation (2.5) and another one contributing to the director field dynamics (2.6). The former captures the stresses that are induced by the molecular motors and propel fluid either inwards or outwards along the filaments if they are either contractile ($\zeta < 0$) or extensile stresses ($\zeta > 0$), respectively, though experiments and microscopic approaches suggest that actomyosin gels are typically contractile [50–53]. The contribution to the director field dynamics either relaxes ($\lambda_1 < 0$) or increases orientation ($\lambda_1 > 0$) over time, the latter having been observed for concentrated actomyosin gels, which show self-alignment effects [12,54]. Both activity contributions depend on the difference $\Delta \chi$ in chemical potential between ATP and its hydrolysis products ADP and inorganic phosphate, as this provides the energy for the molecular motors that induce the motion. These activity terms were introduced by Kruse *et al.* [7] based on symmetry principles, and derived microscopically in [50–53] for active filaments. Similar considerations for active suspensions of self-propelled particles can be found in [1,55].

The molecular field H in (2.6) is the first variation of the Landau–de Gennes energy (2.1) with respect to Q ,

$$H_{ij} = -\frac{\delta \mathcal{F}_{LG}}{\delta Q_{ij}} = a^2 Q_{ij} - c^2 Q_{ij} \text{tr}(Q^2) + \lambda(x) \delta_{ij} + L_1 \partial_k^2 Q_{ij}. \quad (2.9)$$

The Lagrange multiplier $\lambda(x)$ arises from the constraint $\text{tr} Q = 0$. We note that this constraint is equivalent to the normalization condition of the director field, as can be seen by taking the trace of the representation (2.19) for Q . However, taking the trace of equation (2.6), gives, after some

algebra, that $\lambda(x) = -2(\xi + 1)Q_{il}\omega_{li} = 0$, where the last equality follows from $Q_{il} = Q_{li}$. We will therefore drop the $\lambda(x)I$ term from (2.9). The symmetric and antisymmetric parts of the stress tensor σ_{ij} and τ_{ij} that appear in (2.5) are due to the director-flow interaction and have the form

$$\begin{aligned} \sigma_{ij} = & -\xi \left(Q_{ik} + \frac{\delta_{ik}}{2} \right) H_{kj} - \xi H_{ik} \left(Q_{kj} + \frac{\delta_{kj}}{2} \right) \\ & + 2\xi \left(Q_{ij} + \frac{\delta_{ij}}{2} \right) H_{km} Q_{km} - L_1 \partial_j Q_{km} \partial_i Q_{km} \end{aligned} \quad (2.10)$$

$$\tau_{ij} = Q_{ik} H_{kj} - H_{ik} Q_{kj}. \quad (2.11)$$

For future reference, we also introduce the total stress tensor T , which includes all contributions, including those from the active term, that is

$$T_{ij} = -p\delta_{ij} + 2\mu e_{ij} + \tau_{ij} + \sigma_{ij} - \zeta \Delta \chi Q_{ij}. \quad (2.12)$$

We assume that the substrate is impermeable and that the no-slip condition holds for the liquid, hence both components of the liquid vanish at $x_3 = 0$,

$$v = 0. \quad (2.13a)$$

We also impose strong anchoring, so that at $x_3 = 0$, we have

$$Q = Q_1 = q_1(n_1 \otimes n_1 - \frac{1}{2}I), \quad (2.13b)$$

with a given constant $q_1 \in \mathbb{R}$ and $n_1 = [\sin(\theta_1), \cos(\theta_1)] \in \mathbb{R}^2$ (see also [56]).

At the free surface, we use the isotropic surface energy from [48] (retaining only the first constant term),

$$F_s(Q, \nu) = g_0, \quad (2.14)$$

with $\nu(x_1, t)$ denoting the unit normal to the free surface $\eta(x_1, t)$ and g_0 surface tension, which leads to the surface stress (with $I_s \equiv I - \nu \otimes \nu$)

$$T^s = F_s I_s \quad (2.15)$$

that appears in the right-hand side of stress condition at the interface $x_3 = \eta(x_1, t)$

$$v_i T_{ij} = (\delta_{ik} - \nu_i \nu_k) \partial_k T_{ij}^s. \quad (2.16)$$

In addition, we have the kinematic condition

$$\eta_t = v_3 - v_1 \eta_{,1} \quad (2.17)$$

at $x_3 = \eta(x_1, t)$ and we impose the conical anchoring condition on Q , see also [47,57,58],

$$Q = q_2(R(\theta_2)\nu \otimes R(\theta_2)\nu - \frac{1}{2}I), \quad (2.18)$$

with a given constant $q_2 \in \mathbb{R}$ and $\theta_2 \in [0, \pi)$, where

$$R(\theta) = \begin{bmatrix} \cos \theta & \sin \theta \\ -\sin \theta & \cos \theta \end{bmatrix}$$

is the rotation by angle θ_2 . We note, however, that in the thin-film limit derived below in §3, the normal to the free boundary is, to leading order, equal to the canonical unit vector e_3 , hence this boundary condition reduces to a strong anchoring condition with a fixed angle θ_2 with respect to the x_3 -coordinate direction.

(b) Reduction to an active Ericksen model

In this and next sections subscript $_i$ means differentiation with respect to x_i . The reduction of the model (2.4)–(2.6) proceeds as follows: by definition the two eigenvalues of Q are $\pm q/2$ for some

scalar order parameter $q \in \mathbb{R}$. Moreover, one can show that for each $Q \in \mathcal{L}_0$ there exists a unit vector $n \in S^1$ (called director) such that representation

$$Q = q \left[n \otimes n - \frac{I}{2} \right], \quad (2.19)$$

holds. From this, it also follows that each two-dimensional Q -tensor on a plane is completely characterized by two degrees of freedom: the order parameter q and the director n . The representation (2.19) does not distinguish between $+n$ and $-n$. For definiteness, we fix the sign at the free interface, and hence by continuity everywhere in the film, by requiring that n points out of the liquid and the director field is continuous everywhere in the film bulk. In §§4 and 5, we will describe situations when the reduction presented in this section can be extended without changes to the case of singular director fields n having defects.

We note also that under representation (2.19) the bulk energy (2.2) reduces to

$$f_b(Q) = f_b(q) = -\frac{a^2 q^2}{4} + \frac{c^2 q^4}{16}, \quad (2.20)$$

which attains its global minima at $q_{\min} = \pm \sqrt{2}a/c$.

Substituting (2.19) into (2.9) (and taking into account that $\lambda = 0$) one obtains

$$\begin{aligned} H_{ij} = & \left(a^2 q - \frac{c^2 q^3}{2} \right) \left[n_i n_j - \frac{\delta_{ij}}{2} \right] + L_1 q_{,kk} \left[n_i n_j - \frac{\delta_{ij}}{2} \right] \\ & + 2L_1 q_{,k} n_{i,k} n_j + 2L_1 q_{,k} n_i n_{j,k} + L_1 q [2n_{i,k} n_{j,k} + n_{i,kk} n_j + n_i n_{j,kk}]. \end{aligned}$$

On the other hand, expressing of H from (2.6) gives

$$\Gamma H_{ij} = q(n_j N_i + n_i N_j) + (q_t + v_k q_{,k}) \left[n_i n_j - \frac{\delta_{ij}}{2} \right] - S(\nabla v, Q) - \lambda_1 \Delta \chi q \left(n_i n_j - \frac{\delta_{ij}}{2} \right), \quad (2.21)$$

where we denote the rate of change of the director with respect to the background fluid

$$N_i = \dot{n}_i - \omega_{ij} n_j, \quad \dot{n}_i = \partial_t n_i + v_j \partial_j n_i, \quad (2.22)$$

and \dot{n}_i denotes the material derivative.

Calculating the variational quantity $\Gamma(H_{ij} n_j + n_i H_{ij})$ for both of the last two representations for H and subsequently equating them one obtains the following equation:

$$\begin{aligned} L_1 \Gamma [2q n_{i,kk} - 2q |n_{i,k}|^2 n_i + q_{,kk} n_i + 4q_{,k} n_{i,k}] + \Gamma \left(a^2 q - \frac{c^2 q^3}{2} \right) n_i \\ = 2q N_i + (q_t + v_k q_{,k}) n_i - \frac{2}{3} (q + 2) \xi e_{ji} n_j - \lambda_1 \Delta \chi q n_i. \end{aligned} \quad (2.23)$$

Multiplying the last equation by n_i , summing over $i = 1, 3$ and using relations $N_i n_i = n_i^2 - 1 = 0$ one obtains an Allen–Cahn-type equation for the scalar order parameter

$$q_t + v_k q_{,k} - \frac{2}{3} (q + 2) \xi e_{ji} n_j n_i = L_1 \Gamma q_{,kk} - 4q L_1 \Gamma |n_{j,k}|^2 + \Gamma \left(a^2 q - \frac{c^2 q^3}{2} \right) + \lambda_1 \Delta \chi q. \quad (2.24)$$

Using (2.24), one can simplify (2.23) to a parabolic equation for the director field $n(x)$:

$$L_1 \Gamma [2q n_{i,kk} + 4q_{,k} n_{i,k}] = 2q N_i - 2q L_1 \Gamma |n_{j,k}|^2 n_i - \frac{2}{3} (q + 2) \xi [e_{ji} n_j - e_{ik} n_l n_k n_i]. \quad (2.25)$$

The expressions (2.11) and (2.10) for the antisymmetric and symmetric stresses become

$$\Gamma \tau_{ij} = q^2 (n_i N_j - N_i n_j) - \frac{\xi q (q + 2)}{3} (n_i n_k e_{kj} - e_{ik} n_k n_j)$$

$$\begin{aligned} \Gamma \sigma_{ij} = & -\frac{q\xi}{3}(q+2)(n_j N_i + n_i N_j) + \frac{q\xi^2}{3}(4-q)(e_{ik} n_k n_j + n_i n_k e_{kj}) \\ & + \frac{2\xi^2}{3}(q-1)^2 e_{ij} - \frac{8q^2 \xi^2}{3} \left(\frac{3}{4} + q - q^2 \right) \xi n_i n_j e_{ik} n_l n_k \\ & + \frac{\xi q}{2} n_i n_j (q_t + v_k q_{,k}) - \Gamma L_1 \left(\frac{3}{4} q_{,i} q_{,j} + 2q^2 n_{k,i} n_{k,j} \right) \\ & + \xi \lambda_1 \Delta \chi (1 - q^2) q \left(n_i n_j - \frac{\delta_{ij}}{2} \right), \end{aligned}$$

where the last term appears upon inserting expression (2.21) for H_{ij} into (2.10). Finally, we also have the explicit appearance of the active stress in (2.12), $-\zeta \Delta \chi Q_{ij} = -\zeta \Delta \chi q (n_i n_j - \delta_{ij}/2)$, so that the total stress tensor (2.12) becomes

$$T_{ij} = -p \delta_{ij} + T_{ij}^E + \tilde{T}_{ij}, \quad (2.26)$$

$$T_{ij}^E = -L_1 \left(\frac{3}{4} q_{,i} q_{,j} + 2q^2 n_{k,i} n_{k,j} \right) \quad (2.27)$$

$$\begin{aligned} \tilde{T}_{ij} = & \alpha_1 n_k n_p e_{kp} n_i n_j + \alpha_2 N_i n_j + \alpha_3 N_j n_i + \alpha_4 e_{ij} + \alpha_5 e_{ik} n_k n_j + \alpha_6 e_{jk} n_k n_i \\ & + \frac{\xi q}{2\Gamma} n_i n_j (q_t + v_k q_{,k}) + \left[\frac{\xi \lambda_1 (1 - q^2)}{\Gamma} - \zeta \right] \Delta \chi q \left(n_i n_j - \frac{\delta_{ij}}{2} \right). \end{aligned} \quad (2.28)$$

The Leslie constants α_i and the parameters of Beris–Edwards model are related by (see (2.10)–(2.15) in [43])

$$\left. \begin{aligned} \alpha_1(q) &= -\frac{2q^2(3+4q-4q^2)\xi^2}{\Gamma}, & \alpha_2(q) &= \frac{\{-(1/3)q(2+q)\xi - q^2\}}{\Gamma}, \\ \alpha_3(q) &= \frac{\{-(1/3)q(2+q)\xi + q^2\}}{\Gamma}, & \alpha_4(q) &= \frac{4}{9} \frac{(1-q)^2 \xi^2}{\Gamma} + 2\mu, \\ \alpha_5(q) &= \frac{\{(1/3)q(4-q)\xi^2 + (1/3)q(2+q)\xi\}}{\Gamma}, & \alpha_6(q) &= \frac{\{(1/3)q(4-q)\xi^2 - (1/3)q(2+q)\xi\}}{\Gamma}. \end{aligned} \right\} \quad (2.29)$$

We conclude that under representation (2.19) the model (2.4)–(2.6) turns into four equations

$$0 = \partial_i v_i, \quad (2.30a)$$

$$0 = -\partial_i p - L_1 \partial_j \left(\frac{3}{4} q_{,i} q_{,j} + 2q^2 n_{k,i} n_{k,j} \right) + \partial_j \tilde{T}_{ij}, \quad (2.30b)$$

$$L_1 \Gamma [2q n_{i,kk} + 4q_{,k} n_{i,k}] = 2q N_i - 2q L_1 \Gamma |n_{j,k}|^2 n_i - \frac{2}{3} (q+2) \xi [e_{ji} n_j - e_{lk} n_l n_k n_i] \quad (2.30c)$$

and

$$\begin{aligned} q_t + v_k q_{,k} = & \frac{2}{3} (q+2) \xi e_{ji} n_j n_i + L_1 \Gamma q_{,kk} - 4q L_1 \Gamma |n_{j,k}|^2 \\ & + \Gamma \left(a^2 q - \frac{c^2 q^3}{2} \right) + \lambda_1 \Delta \chi q, \end{aligned} \quad (2.30d)$$

where \tilde{T}_{ij} is given by (2.28). As a consistency check, we note that from multiplying (2.30c) by n_i and summing over $i = 1, 3$, one obtains that $d(n_i^2)/dt = 0$ holds for all x and t .

Using (2.19) in (2.13a), the conditions at the substrate $x_3 = 0$ become

$$v_1 = 0, \quad v_3 = 0, \quad n_3 = \cos \theta_1, \quad q = q_1. \quad (2.31)$$

At the free interface $x_3 = \eta(x_1, t)$, we obtain from (2.16)–(2.18) that

$$v_i T_{ij} v_j = -g_0 \partial_i v_i, \quad v_i T_{ij} t_j = 0, \quad \eta_t = v_3 - v_1 \partial_1 \eta, \quad n = R(\theta_2) v, \quad q = q_2. \quad (2.32)$$

3. Derivation of the thin-film models

(a) Thin-film model for the active Erickson theory

We now non-dimensionalize this model using length scales L for x_1 and εL for x_3 , where L denotes the characteristic lateral extent of the cell and εL denote its height. Hence, ε is the ratio between the two length scales and in a thin-film setting assumed to be small. We denote

$$\left. \begin{aligned} x_3 &= \varepsilon L \bar{x}_3, & x_1 &= L \bar{x}_1, & \eta &= \varepsilon L \bar{\eta}, \\ v_1 &= U \bar{v}_1, & v_3 &= \varepsilon U \bar{v}_3, & t &= \left(\frac{L}{U}\right) \bar{t}, \\ p &= p_0 + P \bar{p}, & h &= \mathcal{E} \bar{h}, \end{aligned} \right\} \quad (3.1)$$

and

where \mathcal{E} and P are defined as

$$\mathcal{E} = \frac{L_1}{\varepsilon^2 L^2} \quad \text{and} \quad P = \frac{\mu U}{\varepsilon^2 L}. \quad (3.2)$$

The order parameter q and the director field n are dimensionless and do not need to be scaled. In the normal stress condition at the free surface, balancing the pressure with surface tension requires $P = \varepsilon g_0/L$. Together with the choice for P in (3.2) this means

$$\varepsilon^3 = \frac{\mu U}{g_0}. \quad (3.3)$$

Further scalings are

$$\left. \begin{aligned} N_i &= \frac{U}{\varepsilon L} \bar{N}_i, & e_{11} &= \frac{U}{L} \bar{e}_{11}, & e_{13} &= \frac{U}{\varepsilon L} \bar{e}_{13}, & e_{31} &= \frac{U}{\varepsilon L} \bar{e}_{31}, & e_{33} &= \frac{U}{L} \bar{e}_{33}, \\ \omega_{13} &= \frac{U}{\varepsilon L} \bar{\omega}_{13}, & \omega_{31} &= \frac{U}{\varepsilon L} \bar{\omega}_{31}, & \alpha_i &= \mu \bar{\alpha}_i, & \Gamma &= \frac{\bar{\Gamma}}{\mu}, & a^2 &= \mathcal{E} \bar{a}^2, & c^2 &= \mathcal{E} \bar{c}^2, \\ \tilde{T}_{ij} &= \frac{\mu U}{\varepsilon L} \bar{\tilde{T}}_{ij}, & [T_{11}^E, T_{13}^E, T_{31}^E, T_{33}^E] &= \frac{\mu U}{\varepsilon L} [\varepsilon^2 \bar{T}_{11}^E, \varepsilon \bar{T}_{13}^E, \varepsilon \bar{T}_{31}^E, \bar{T}_{33}^E] \end{aligned} \right\} \quad (3.4)$$

and

$$\bar{L}_1 = \frac{L_1}{\varepsilon \mu U L}, \quad \bar{\zeta} \Delta \bar{\chi} = \frac{\Gamma L}{U} \zeta \Delta \chi, \quad \bar{\lambda}_1 \Delta \bar{\chi} = \frac{L}{U} \lambda_1 \Delta \chi.$$

Retaining only the leading-order terms in ε in the rescaled system (2.20), given in appendix A, and assuming the weak elasticity limit, by which we mean that as we introduce the thin-film approximation $\varepsilon \rightarrow 0$, we assume $\bar{L}_1 = O(1)$ and $\Delta \bar{\chi} = O(\varepsilon^{-1})$, the leading-order system in the bulk becomes (with $(i, j) = (1, 3)$ and $(i, j) = (3, 1)$ used below)

$$0 = v_{1,1} + v_{3,3}, \quad (3.5a)$$

$$0 = -p_{,1} + \frac{1}{2}(v_{1,3} f_A(n_1, n_3))_{,3} + \frac{\varepsilon}{\Gamma} \Delta \chi [(\xi \lambda_1 (1 - q^2) - \zeta) q n_{1,3}]_{,3}, \quad (3.5b)$$

$$0 = -p_{,3}, \quad (3.5c)$$

$$\begin{aligned} q n_{i,33} + 2q_{,3} n_{i,3} &= -q \frac{v_{1,3} n_j}{2L_1 \Gamma} - q (|n_{1,3}|^2 + |n_{3,3}|^2) n_i \\ &\quad - \frac{v_{1,3}}{3L_1 \Gamma} (q + 2) \xi \left[\frac{n_i}{2} - n_i^2 n_j \right] \end{aligned} \quad (3.5d)$$

and

$$\begin{aligned} -\frac{2}{3} (q + 2) \xi v_{1,3} n_1 n_3 &= -4q L_1 \Gamma (|n_{1,3}|^2 + |n_{3,3}|^2) + L_1 \Gamma q_{,33} \\ &\quad + \Gamma \left(a^2 q - \frac{c^2 q^3}{2} \right) + \varepsilon \lambda_1 \Delta \chi q, \end{aligned} \quad (3.5e)$$

where here and below for convenience we have skipped the overbars everywhere and in the horizontal momentum equation we introduced the notation

$$f_A(n_1, n_3) \equiv 2\alpha_1(n_1 n_3)^2 + (\alpha_5 - \alpha_2)n_3^2 + (\alpha_3 + \alpha_6)n_1^2 + \alpha_4. \quad (3.6)$$

The leading-order system for the boundary conditions at $z = 0$ is given by

$$v_1 = 0, \quad v_3 = 0, \quad n_3 = \cos \theta_1, \quad q = q_1, \quad (3.7)$$

and at the free surface, $x_3 = \eta(x_1, t)$ by

$$\left. \begin{aligned} \eta_t &= v_3 - v_1 \partial_1 \eta, \\ -p &= \eta_{,11}, \quad \frac{1}{2} v_{1,3} f_B(n_1, n_3) = -\frac{\varepsilon}{\Gamma} \Delta \chi (\xi \lambda_1 (1 - q^2) - \zeta) q n_3 n_1 \end{aligned} \right\} \quad (3.8)$$

and

$$n_3 = \cos \theta_2, \quad q = q_2,$$

with a given function $q_2(x, t)$, and where we define

$$f_B(n_1, n_3) \equiv 2\alpha_1(n_1 n_3)^2 + (\alpha_6 - \alpha_3)n_3^2 + (\alpha_2 + \alpha_5)n_1^2 + \alpha_4. \quad (3.9)$$

Next, similar to [17] we rewrite equations ((3.5a)–e) in the bulk in terms of the director angle θ using the representation $n_1 = \sin \theta$, $n_3 = \cos \theta$. For that, we multiply (3.5d) for $(i, j) = (1, 3)$ by $-n_3$ and for $(i, j) = (3, 1)$ by n_1 and then sum the resulting equations up. With the definitions

$$\gamma_1 = \alpha_3 - \alpha_2, \quad \gamma_2 = \alpha_2 + \alpha_3 = \alpha_6 - \alpha_5 \quad (3.10)$$

and (2.29) we thus obtain for ((3.5a)–e)

$$0 = v_{1,1} + v_{3,3}, \quad (3.11)$$

$$0 = -p_{,1} + \frac{1}{2} (v_{1,3} f_A(q, \theta))_{,3} + \frac{\varepsilon}{2\Gamma} \Delta \chi [(\xi \lambda_1 (1 - q^2) - \zeta) q \sin(2\theta)]_{,3}, \quad (3.12)$$

$$0 = -p_{,3}, \quad (3.13)$$

$$(q^2 \theta_{,3})_{,3} = -\frac{v_{1,3}}{4L_1} [\gamma_1 - \gamma_2 \cos(2\theta)] \quad (3.14)$$

$$\text{and} \quad -\frac{1}{3} (q + 2) \xi v_{1,3} \sin(2\theta) = -4qL_1 \Gamma |\theta_{,3}|^2 + L_1 \Gamma q_{,33} + \Gamma \left(a^2 q - \frac{c^2 q^3}{2} \right) + \varepsilon \lambda_1 \Delta \chi q, \quad (3.15)$$

where we have defined

$$f_A(q, \theta) = \left(\frac{\alpha_1}{2} \right) \sin^2(2\theta) + (\alpha_5 - \alpha_2) \cos^2 \theta + (\alpha_3 + \alpha_6) \sin^2 \theta + \alpha_4. \quad (3.16)$$

The leading-order system for the boundary conditions at $z = 0$ is given by

$$v_1 = 0, \quad v_3 = 0, \quad \theta = \theta_1, \quad q = q_1, \quad (3.17)$$

and at the free surface, $x_3 = \eta(x_1, t)$ by

$$\left. \begin{aligned} -p &= \eta_{,11}, \quad \frac{1}{2} v_{1,3} f_B(q, \theta) = -\frac{\varepsilon}{2\Gamma} \Delta \chi (\xi \lambda_1 (1 - q^2) - \zeta) q \sin(2\theta) \\ \eta_t &= v_3 - v_1 \partial_1 \eta, \quad \theta = \theta_2, \quad q = q_2, \end{aligned} \right\} \quad (3.18)$$

where we define

$$f_B(q, \theta) = \left(\frac{\alpha_1}{2} \right) \sin^2(2\theta) + (\alpha_6 - \alpha_3) \cos^2 \theta + (\alpha_2 + \alpha_5) \sin^2 \theta + \alpha_4. \quad (3.19)$$

We now integrate these equations. From (3.12) and (3.13), and the stress boundary conditions in (3.18), we get $p = -\eta_{,11}$ and

$$f_A(q, \theta)v_{1,3} = 2\eta_{,111}(\eta - x_3) - \frac{\varepsilon}{\Gamma} \Delta \chi (\xi \lambda_1 (1 - q^2) - \zeta) q \sin(2\theta) + \frac{\varepsilon}{\Gamma} \Delta \chi \frac{\gamma_1 - \gamma_2 \cos(2\theta_2)}{f_B(q_2, \theta_2)} (\xi \lambda_1 (1 - q_2^2) - \zeta) q_2 \sin(2\theta_2), \quad (3.20)$$

provided $f_B(q_2, \theta_2) \neq 0$. Together with the integrated mass conservation equation (which we note is exact, i.e. valid also for the full governing equations) that we obtain by combining (3.11) and the kinematic equation in (3.18) we arrive at the *lubrication system*

$$\eta_t(x_1, t) = -\partial_1 \int_0^\eta v_1(x_1, x_3, t) dx_3, \quad (3.21a)$$

$$v_{1,3} = \frac{2\eta_{,111}}{f_A(q, \theta)} (\eta - x_3) - \frac{\varepsilon \Delta \chi}{\Gamma f_A(q, \theta)} \left[(\xi \lambda_1 (1 - q^2) - \zeta) q \sin(2\theta) - \frac{\gamma_1 - \gamma_2 \cos(2\theta_2)}{f_B(q_2, \theta_2)} (\xi \lambda_1 (1 - q_2^2) - \zeta) q_2 \sin(2\theta_2) \right], \quad (3.21b)$$

$$(q^2 \theta_{,3})_{,3} = -\frac{1}{4L_1} (\gamma_1 - \gamma_2 \cos(2\theta)) v_{1,3} \quad (3.21c)$$

and
$$q_{,33} = 4q(\theta_{,3})^2 - \frac{\xi(q+2)}{3L_1\Gamma} \sin(2\theta) v_{1,3} - \frac{q}{L_1} \left(a^2 - \frac{c^2 q^2}{2} \right) - \frac{\varepsilon \lambda_1 \Delta \chi}{L_1 \Gamma} q. \quad (3.21d)$$

Note that if $f_A(q, \theta) \neq 0$ for all x_1, x_3 and t , we can substitute (3.21b) into (3.21c) and (3.21d) to eliminate $v_{1,3}$, thus decoupling the system for θ and q from the velocity field. We have not done this here for clarity. The system is complemented by the following boundary conditions:

$$\text{and} \quad \left. \begin{aligned} v_1 = 0, \quad \theta = \theta_1, \quad q = q_1, \quad \text{at } x_3 = 0 \\ \theta = \theta_2, \quad q = q_2, \quad \text{at } x_3 = \eta. \end{aligned} \right\} \quad (3.21e)$$

(b) Thin-film model for the active Leslie–Erickson–Parodi theory

If we use the Leslie–Erickson–Parodi theory with corresponding active terms as a model for the active liquid crystal [7,8,12,13] and non-dimensionalize as before we derive in appendix B the following coupled system for the leading-order thin-film approximation

$$\partial_t \eta = -\partial_1 \int_0^\eta v_1 dx_3, \quad (3.22a)$$

$$0 = \eta_{,111}(x_3 - \eta) + \frac{1}{2} v_{1,3} f_A(\theta) + \frac{\zeta^* \Delta \chi^* f_A(\theta_2)}{2 f_B(\theta_2)} \sin(2\theta_2) + \frac{\zeta^* \Delta \chi^*}{2} (\sin(2\theta) - \sin(2\theta_2)) \quad (3.22b)$$

and
$$2K\theta_{,33} = -(\gamma_1 - \gamma_2 \cos(2\theta)) v_{1,3}, \quad (3.22c)$$

with the boundary conditions

$$\text{and} \quad \left. \begin{aligned} v_1 = 0, \quad \theta = \theta_1 \quad \text{at } x_3 = 0 \\ \theta = \theta_2 \quad \text{at } x_3 = \eta(x_1, t). \end{aligned} \right\} \quad (3.23)$$

Formal comparison of (3.22) with equations ((3.21a)–c) considered with $q = q_1 = q_2 = \text{const.}$ provides the following relations between the active and elastic parameters in the Eriksen–Leslie–Parodi and Eriksen thin-film models:

$$\lambda_1^* = \lambda_1, \quad \zeta^* = (\zeta - \xi \lambda_1 (1 - q^2)) q, \quad K = 2L_1 q^2, \quad \Delta \chi^* = \frac{\varepsilon}{\Gamma} \Delta \chi. \quad (3.24)$$

Though λ_1^* does not appear in the reduced thin-film model (3.22), it is important to highlight its relation to λ_1 , because the latter does appear in the q -equation (3.21d) of the extended model (3.21). At the same time, in the absence of the active terms $\Delta\chi^* = 0$ our model (3.22) can be shown to coincide with the (passive) thin-film model derived in [17] for the weak elasticity regime, cf. system (A17)–(A20) therein. Note that the special anchoring boundary conditions $\theta_1 = \pi/2$ and $\theta_2 = 0$ were considered in Lin *et al.* [17].

4. Impact of activity terms

At this point, further reductions of the thin-film models (3.21) or (3.22) are not, in general, possible without additional assumptions, since the remaining equations cannot be easily integrated with respect to x_3 . We will instead look at two special cases of the more general Q -tensor system (3.21): one, where the interface is flat ($\eta = 1$) and the other where the misalignment of the director at the substrate and the interface is small, $|\theta_2 - \theta_1| \ll 1$.

(a) Flat film

We first consider the passive case, where also $\eta = \text{const.}$ is any positive constant. This yields $v_1 = 0$ and

$$q^2\theta_{,3} = c_1, \quad q_{,33} = 4q(\theta_{,3})^2 - \frac{1}{L_1} \left(a^2q - \frac{c^2q^3}{2} \right). \quad (4.1)$$

Under the additional assumption that $q_1 = q_2 \equiv q_0$ and that q remains constant, we obtain the solution

$$\theta = (\theta_2 - \theta_1) \frac{x_3}{\eta} + \theta_1, \quad q = q_0 = \left[\frac{2a^2}{c^2} - \frac{8L_1}{c^2} (\theta_2 - \theta_1)^2 \right]^{1/2}. \quad (4.2)$$

We note that a similar solution for the director angle θ and for q has been found for the case of channel flow in [40].

Alternatively, one can also combine the equations in (4.1) to obtain one ODE for q , which, after multiplying with $q_{,3}$ and integrating once reads

$$\frac{1}{2}q_{,3}^2 = -\frac{2c_1^2}{q^2} - \frac{1}{L_1} \left(\frac{a^2}{2}q^2 - \frac{c^2q^4}{8} \right) + c_2, \quad (4.3)$$

where we have assumed that $q \neq \text{const.}$ and c_2 is an integration constant. The last ODE is separable and can be integrated as

$$x_3 = \int_{q_1}^q \frac{ds}{\sqrt{-4c_1^2/s^2 - (1/L_1)(a^2s^2 - c^2s^4/4) + 2c_2}}, \quad (4.4)$$

where we have assumed that $q_2 > q_1$. Correspondingly, using the first equation in (4.1) one gets

$$\theta(x_3) - \theta_1 = c_1 \int_{q_1}^q \frac{ds}{s^2 \sqrt{-4c_1^2/s^2 - (1/L_1)(a^2s^2 - c^2s^4/4) + 2c_2}}. \quad (4.5)$$

The constants c_1 and c_2 are determined by the boundary condition for θ at $x_3 = \eta = \text{const.}$:

$$\left. \begin{aligned} \theta_2 - \theta_1 &= \int_{q_1}^{q_2} \frac{(c_1/s^2) ds}{\sqrt{-4c_1^2/s^2 - (1/L_1)(a^2s^2 - c^2s^4/4) + 2c_2}} \\ \text{and} \quad \eta &= \int_{q_1}^{q_2} \frac{ds}{\sqrt{-4c_1^2/s^2 - (1/L_1)(a^2s^2 - c^2s^4/4) + 2c_2}} \end{aligned} \right\} \quad (4.6)$$

Two nonlinear compatibility conditions (4.6) may have multiple solutions or do not have ones at all depending on the given set of four parameters $q_1, q_2, \theta_1 - \theta_2$ and η . In the latter case, there exists

only one trivial solution (4.2) to system (4.1). We aim to investigate existence and multiplicity parameter regions for solutions to (4.6) in a subsequent study.

For an active flat film the compatibility condition of $\eta(x_1, x_3, t) = \eta = \text{const.}$ with (3.21a) implies that v_1, q, θ are functions of x_3 only. By that, system ((3.21b)–d) reduces to

$$v_{1,3} = -\frac{\varepsilon \Delta \chi}{\Gamma f_A(q, \theta)} \left[(\xi \lambda_1 (1 - q^2) - \zeta) q \sin(2\theta) - \frac{\gamma_1 - \gamma_2 \cos(2\theta_2)}{f_B(q_2, \theta_2)} (\xi \lambda_1 (1 - q_2^2) - \zeta) q_2 \sin(2\theta_2) \right] \quad (4.7a)$$

$$(q^2 \theta_{,3})_{,3} = -\frac{1}{4L_1} (\gamma_1 - \gamma_2 \cos(2\theta)) v_{1,3} \quad (4.7b)$$

and
$$q_{,33} = 4q(\theta_{,3})^2 - \frac{\xi(q+2)}{3L_1 \Gamma} \sin(2\theta) v_{1,3} - \frac{q}{L_1} \left(a^2 - \frac{c^2 q^2}{2} \right) - \frac{\varepsilon \lambda_1 \Delta \chi}{L_1 \Gamma} q, \quad (4.7c)$$

which further reduce to two coupled ODEs for $\theta(x_3)$ and $q(x_3)$ by eliminating $v_{1,3}$. The latter ODEs can be effectively integrated numerically.

Note, that in the absence of the active terms ($\lambda_1 = 0$ or $\zeta = 0$) the non-trivial solution to the system (4.7) is given by (4.4) and (4.5) combined with $v_1 = 0$ and it exists only when the compatibility conditions (4.6) for the boundary data (3.21e) are satisfied. Given $q_2 > q_1$, such that the square root in the denominator of (4.4) is real for all $q \in (q_1, q_2)$, by taking η and $\theta_2 - \theta_1$ sufficiently large, one can realize this passive solution. Moreover, also for small active terms with $\Delta \chi \ll 1$ this non-homogeneous solution to the system (4.7) continuously persists and by (4.7a) exhibits the non-homogeneous flow $v_1(x_3)$ with $|v_1| \ll 1$. This effect of inducing a non-zero flow in a channel geometry, when the thickness of the latter η becomes sufficiently large, has been observed in [9,12] for the polar LEP-based models.

Finally, note that when active terms are present in (4.7) there is no analogous solution to (4.2), i.e. having constant $q(x_3) = q_0$. In this case, three equations ((4.7a)–b) are not compatible, unless the trivial isotropic case $q_0 = 0$ holds. By contrast, the passive solution (4.2) to LEP model (3.22) having initially the linear director profile can be continued also in the presence active terms. These solutions can be found numerically or analytically as ones to the corresponding active stationary system:

$$0 = \frac{1}{2} v_{1,3} f_A(\theta) + \frac{\zeta^* \Delta \chi^* f_A(\theta_2)}{2 f_B(\theta_2)} \sin(2\theta_2) + \frac{\zeta^* \Delta \chi^*}{2} (\sin(2\theta) - \sin(2\theta_2)) \quad (4.8a)$$

and
$$2K\theta_{,33} = -(\gamma_1 - \gamma_2 \cos(2\theta)) v_{1,3}, \quad (4.8b)$$

considered with boundary conditions (3.23).

(b) Film with small angle change in the director boundary condition

Another special case, where it is possible to discuss analytical solutions is obtained if the difference in the director angle is small.

We first consider the passive case. Assuming $|\theta_2 - \theta_1| \ll 1$, then to leading order $\theta = \theta_2 = \theta_1$ is constant and (3.21c) implies $v_{1,3} = v_1 = 0$ and $\eta = \text{const.}$ As a result, the whole dynamics reduces to (3.21d), which can be further reduced to (4.3) with $c_1 = 0$. Then the corresponding solution is given by

$$x_3 = - \int_{q_1}^{q(x_3)} \frac{ds}{\sqrt{-(1/L_1)(a^2 s^2 - c^2 s^4/4) + 2c_2}} \quad \text{for } x_3 \in (0, \eta). \quad (4.9)$$

The compatibility conditions (4.6) reduce to

$$\eta = - \int_{q_1}^{q_2} \frac{ds}{\sqrt{-(1/L_1)(a^2 s^2 - c^2 s^4/4) + 2c_2}}. \quad (4.10)$$

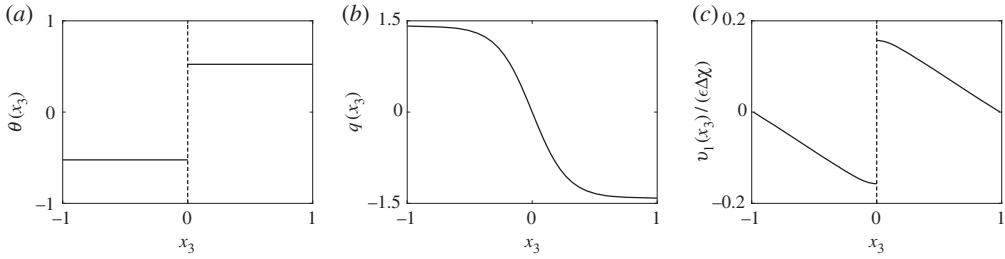


Figure 2. Director angle profile (a) and q -profile (b) for the solution (4.9), (4.11) with $\theta_1 = -\pi/6, \theta_2 = \pi/6, a = 1, c = 1, \eta = 1, L_1 = 0.04$ and $c_2 = 12.507$ calculated numerically. (c) leading-order velocity profile (4.12) (normalized by $\varepsilon \Delta \chi \ll 1$) corresponding to the continued solution (4.9), (4.11) in the active case with $\zeta = \Gamma = \mu = 1$ and $\xi = 0$.

As an important illustration of the difference between Ericksen (3.21) and LEP (3.22) models, we point out that the new solution (4.9) can be used as a building block for construction of admissible solutions with discontinuous director field $\theta(x_3)$. Namely, let us consider the particular case $q_1 = -q_{\min} = \sqrt{2}a/c < q_2 = 0$, in (4.9) and (4.10). Then it is easy to show existence of a unique $c_2(\eta)$ satisfying (4.6). We can extend (4.9) by a reflection around $x_3 = 0$ as

$$\theta(x_3) = -\theta_1, \quad x_3 = - \int_0^{q(x_3)} \frac{ds}{\sqrt{-(1/L_1)(a^2s^2 - c^2s^4/4) + 2c_2}} \quad \text{for } x_3 \in (-\eta, 0), \quad (4.11)$$

now with $q_1 = q_{\min} = \sqrt{2}a/c > q_2 = 0$. The resulting combined solution (4.9), (4.11) (figure 2a,b) is a suitably defined weak solution to stationary system (4.1) considered in the interval $(-\eta, \eta)$. Accordingly, the defect line $x_3 = 0$ is isotropic with $q(0) = 0$ and across it the director jumps by value $2\theta_1$. Additionally, we note that the constructed solution (4.9), (4.11) corresponds to the limiting profile as the elastic constant tends to zero of the antisymmetric nematic field in the channel observed numerically in [40], cf. in particular with approximate formula (29) therein.

The solution (4.9), (4.11) occurs also as a solution to the system (4.7) in the presence of small active terms, i.e. when $0 < \varepsilon \Delta \chi \ll 1$. In this case, a non-zero flow is generated, such that the fluid moves in the bottom and upper half of the channel but in opposite directions prescribed by the director field (figure 2c). Indeed, if we consider for simplicity the case $\xi = 0$, then (4.7a) reduces to

$$v_{1,3} = \frac{\varepsilon \zeta \Delta \chi}{q^2 + 2\Gamma \mu} q \sin(2\theta). \quad (4.12)$$

Substituting (4.9) and (4.11) into the right-hand side of (4.12) and applying no-slip boundary conditions at $x = \pm \eta$ one obtains (4.12) as the explicit leading order outer solution for $v_1(x_3)$ for $\varepsilon \Delta \chi$, which is an odd function of x_3 (figure 2c). We conjecture that there exist material parameter regimes for which (4.12) can be smoothly matched to an inner solution at $x_3 = 0$. Together with (4.9), (4.11), this results in a solution of the active system (4.7). Note that the jump singularity of the θ -profile (figure 2a) is also expected to be smoothed out in the vicinity of $x_3 = 0$.

Another way to initiate a non-trivial dynamics in the case $\theta = \theta_2 = \theta_1 = \text{const.}$ is to assume

$$\gamma_1 - \gamma_2 \cos(2\theta) = 0. \quad (4.13)$$

This would imply that (3.21c) is satisfied and $q = q_1 = q_2 = \text{const.}$ Furthermore, (3.21b) can be integrated and introduced into (3.21a) yields a new modified thin-film equation

$$\eta_t = - \frac{2}{3f_A(q_1, \theta_1)} \partial_1(\eta^3 \eta_{,111}) + C(q_1, \theta_1) \partial_1(\eta^2). \quad (4.14)$$

Note that in this case, besides the trivial isotropic solution $q_1 = 0$, only special values of q_1 and θ_1 are allowed. These have to be compatible with both, equation (4.13) and the algebraic relation

$$0 = \left(a^2 - \frac{c^2 q^2}{2} \right) + \frac{\varepsilon \lambda_1 \Delta \chi}{\Gamma}. \quad (4.15)$$

which arises from (3.21d).

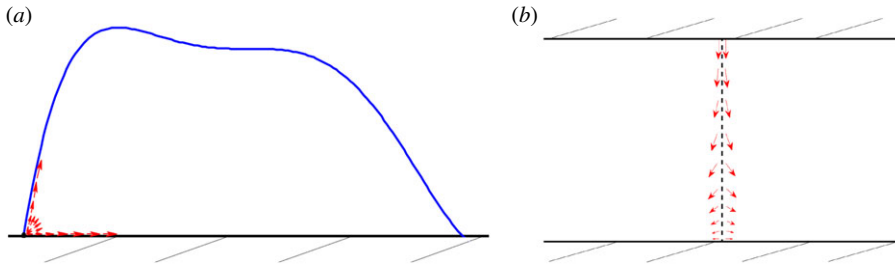


Figure 3. Examples of defects of rotational degree 1 at the contact line (a) and a wall defect (b), which is described by the point defect of degree -1 located at the intersection of the wall (depicted by dashed line) and the substrate. The director field in the defect neighbourhood is shown by arrows. Magnitude of scalar order parameter q is represented by arrow sizes. Lubrication model (3.21) smoothly resolves such defects through reduction to $q = 0$ in their vicinity. (Online version in colour.)

For given activity $\lambda_1 \Delta \chi \in \mathbb{R}$, solutions for q_1 and θ_1 can be obtained from (4.13) and (4.15) as

$$\cos(2\theta) = -\frac{3}{\xi} + \frac{6}{(2+q)\xi} \quad \text{and} \quad q^2 = \frac{2a^2}{c^2} + \frac{2\varepsilon\lambda_1\Delta\chi}{c^2\Gamma}. \quad (4.16)$$

Finally, note that solution (4.16) to system (3.21) does not always exist. In particular, it does not exist for $\xi = 0$, i.e. when liquid crystal molecules align perfectly with the hydrodynamic flow. In the absence of active terms ($\lambda_1 = 0$ or $\zeta = 0$), one has $C(q_1, \theta_1) = 0$ in (4.14), and therefore the hydrodynamic flow decouples from the nematics via the rescaling of time by $f_A(q_1, \theta_1)$.

5. Discussion and outlook

In this article, we presented a systematic asymptotic derivation of the thin-film model given by the system (3.21) from the free-boundary problem for the Beris–Edwards model (2.4)–(2.6) to describe the evolution and flow structure of an active nematic liquid crystal. We also showed that the new thin-film model formally reduces to the polar one (3.22) based on LEP theory, when the scalar order parameter q is homogeneous, which in the passive case coincides with the model derived previously in [17]. In the active case, the steady-state solution to (3.21) considered in §4a exhibits non-zero flow that can be spontaneously initiated from the homogeneous one by increasing the film thickness, as previously observed in [9,12].

Additionally, we were able to construct a passive steady state with discontinuous director field in §4 and figure 2. In the Ericksen theory, the defects are defined as singular points where the scalar order parameter $q = 0$ [23]. We note, that besides the singularities of the director field the solutions to (3.21) may exhibit singular lines along which $q = 0$ but n is still continuous. These lines have special physical meaning, because the Q -tensor in (2.19) is zero and, therefore, the nematic field is isotropic along them. A typical example of such a line is given by the middle line of the channel at the right embedded Q -tensor plot in fig. 2 of [40]. Our discontinuous solution can be considered as the limiting profile for that one of [40] as the elastic constant tends to zero.

In summary, both passive and active solutions derived in §4 for nematic (3.21) and polar (3.22) thin-film models can potentially find important applications to design and development of microfluidic devices (cf. review [59]).

We now point to some further applications as well as extensions of our results. The derivation of the coupled model (3.21) starting from the Ericksen-type model (2.20) considered with boundary conditions (2.31) and (2.32) has been conveyed under the assumption of continuity of the director field n in the film bulk and at the free surface. We note that these models are capable to describe solutions having point defects of integer rotational degree k with $k \in \mathbb{Z}$. Two typical examples of defects with degree -1 in the film bulk and of degree 1 at the film contact line are presented in figure 3. One observes that when approaching the defect points the magnitude of the scalar order parameter q goes to zero and by that preserves the continuity of the full Q -tensor field (2.19). We should also point out that, being derived in the weak elasticity regime (cf. scaling

for L_1 in (3.4)) and under the large pressure scaling P in (3.2), the model (3.21a), (3.21) allows for $O(1)$ variation of the director field n along the vertical x_3 -direction of the film. This is the case, for example, in the wall defect of degree -1 in a confined flat film presented in figure 3b, where the director angle θ changes from 0 to $\pi/2$ along the vertical film direction. Such wall defects were observed before in experiments on thin passive nematic films [60].

However, the Ericksen model may not always resolve defects of rational degree $k + 1/2, k \in \mathbb{Z}$, because the latter exhibit special disclination curves along which n changes to $-n$ [49,61,62]. Nevertheless, such defects can be described by the lubrication model (3.21) if the special condition

$$\lim_{(x_1, x_3) \rightarrow (x_1^*, x_3^*)} |\sqrt{q(x_1, x_3)} \nabla n(x_1, x_3)| < \infty, \quad (5.1)$$

is fulfilled, where (x_1^*, x_3^*) is an instant defect location. It is easy to check that (5.1) ensures then that the associated local Ericksen elastic energy [38] and the corresponding terms involving director gradients in (3.21c, d) are kept finite.

Even a spreading of droplet of a passive liquid crystal can exhibit defects that cannot be resolved by a thin-film theory based on Leslie–Ericksen theory [18], and a tensorial theory is required. This is a fortiori true for droplets of active matter [63]. Singularities occur generically at the contact-line, where the anchoring conditions usually clash, or we may have defects in the bulk of the droplet, for example, horizontally aligned vortices, asters or half-defects, which may be tested against experiments with suspensions of active particles (see [63] and references therein). Note that these defects also play an important role in the *in vitro* experiments with actin filaments mentioned earlier [10,11]. The thin-film model developed here based on the Ericksen theory with an additional order parameter for the degree or anisotropy represents the basis to reliably capture these situations and the defects. It will need to be extended to three dimensions, so that horizontally aligned defects can be treated. Other parameter regimes, such as the case of moderate elasticity, where the director field decouples from the flow [17] will be of interest.

Finally, we note that by imposing the constant scalar order parameter $q = q_2$ in (2.18) we neglected possible Marangoni effects at the free surface in the second condition in (2.32). This was motivated by the fact that under the balance (3.3) that keeps the surface tension term at leading order in the normal stress condition (that is, the first equation in (2.32)), the equation for the Marangoni force (e.g. formula (8) in [48]) necessarily implies that q should be constant at the film free surface. Nevertheless, by relaxing condition (3.3) and neglecting surface tension one would be able to derive a model analogous to (3.21) for pure Marangoni driven active nematic thin films.

Data accessibility. This article has no additional data.

Authors' contributions. G.K., A.M. and B.W. all conceived and contributed to the development of the mathematical models and the writing of the manuscript equally.

Competing interests. We have no competing interests.

Funding. G.K. would like to acknowledge support from Leverhulme grant no. RPG-2014-226.

Acknowledgements. The authors thank Jonathan Robbins, Valeriy Slastikov and Arghir Zarnescu for their valuable comments on the results of this article. G.K. gratefully acknowledges the hospitality of the Weierstrass-Institute Berlin during his research visit.

Appendix A. Scaled equations for the active Ericksen system

In this section, we use the convention that $(i, j) = (1, 3)$ or $(i, j) = 3, 1$ and do not use the Einstein's summation convention. Moreover, $\varepsilon_i = \varepsilon$ and 1 if $i = 1$ and $i = 3$, respectively. After application of the scalings (3.1)–(3.4) and dropping the overbars, the bulk equations (2.20) for the Ericksen system take the form

$$\begin{aligned} 0 &= v_{1,1} + v_{3,3}, \\ 0 &= -p_i - \varepsilon^3 T_{i1,1}^E - \varepsilon T_{i3,3}^E + \varepsilon \tilde{T}_{i1,1} + \tilde{T}_{i3,3}, \end{aligned}$$

$$\begin{aligned}
& L_1 \Gamma (2\varepsilon^2 q n_{i,11} + 2q n_{i,33} + 4\varepsilon^2 q_{,1} n_{i,1} + 4q_{,3} n_{i,3}) \\
&= 2q N_i - 2q L_1 \Gamma (\varepsilon^2 |n_{1,1}|^2 + |n_{1,3}|^2 + \varepsilon^2 |n_{3,1}|^2 + |n_{3,3}|^2) n_i \\
&- \frac{2}{3} (q + 2) \xi (\varepsilon_i e_{11} n_i + \varepsilon_j e_{33} n_j - (\varepsilon e_{11} n_1 n_1 + e_{13} n_1 n_3 + e_{31} n_3 n_1 + \varepsilon e_{33} n_3 n_3) n_i), \\
&\varepsilon (q_t + v_k q_{,k}) - \frac{2}{3} (q + 2) \xi (\varepsilon e_{11} n_1 n_1 + e_{13} n_1 n_3 + e_{31} n_3 n_1 + \varepsilon e_{33} n_3 n_3) \\
&= -4q L_1 \Gamma (\varepsilon^2 |n_{1,1}|^2 + |n_{1,3}|^2 + \varepsilon^2 |n_{3,1}|^2 + |n_{3,3}|^2) \\
&+ L_1 \Gamma (\varepsilon^2 q_{,11} + q_{,33}) + L_1 \Gamma \left(a^2 q - \frac{c^2 q^3}{2} \right) + \varepsilon \lambda_1 \Delta \chi q,
\end{aligned}$$

where

$$\begin{aligned}
T_{ii}^E &= L_1 \left[\frac{3}{4} |q_{,i}|^2 + 2q^2 (|n_{1,i}|^2 + |n_{3,i}|^2) \right], \quad T_{ij}^E = L_1 \left[\frac{3}{4} q_{,1} q_{,3} + 2q^2 (n_{1,1} n_{1,3} + n_{3,1} n_{3,3}) \right], \\
\tilde{T}_{ii} &= \alpha_1 (\varepsilon n_1 n_1 e_{11} + n_1 n_3 e_{13} + n_3 n_1 e_{31} + \varepsilon n_3 n_3 e_{33}) n_i n_i + \alpha_2 N_i n_i + \alpha_3 N_j n_j + \alpha_4 \varepsilon e_{ii} \\
&+ \alpha_5 (\varepsilon_i e_{11} n_1 n_i + \varepsilon_j e_{33} n_3 n_j) + \alpha_6 (\varepsilon_i e_{11} n_1 n_i + \varepsilon_j e_{33} n_3 n_j) \\
&+ \frac{\varepsilon}{\Gamma} \frac{\xi q}{2} n_i n_i (q_t + v_1 q_{,1} + v_3 q_{,3}) + \frac{\varepsilon}{\Gamma} [\xi \lambda_i (1 - q^2) - \zeta] \Delta \chi q \left(n_i n_i - \frac{1}{2} \right), \\
\tilde{T}_{ij} &= \alpha_1 (\varepsilon n_1 n_1 e_{11} + n_1 n_3 e_{13} + n_3 n_1 e_{31} + \varepsilon n_3 n_3 e_{33}) n_1 n_3 + \alpha_2 N_i n_j + \alpha_3 N_j n_i + \alpha_4 \varepsilon e_{ij} \\
&+ \alpha_5 (\varepsilon_i e_{11} n_1 n_j + \varepsilon_j e_{33} n_3 n_j) + \alpha_6 (\varepsilon_j e_{33} n_3 n_j + \varepsilon_i e_{11} n_1 n_i) \\
&+ \frac{\varepsilon}{\Gamma} \frac{\xi q}{2} n_1 n_3 (q_t + v_1 q_{,1} + v_3 q_{,3}) + \frac{\varepsilon}{\Gamma} [\xi \lambda_1 (1 - q^2) - \zeta] \Delta \chi q n_1 n_3, \\
e_{ii} &= \partial_i v_i, \quad e_{ij} = \frac{1}{2} (\partial_3 v_1 + \varepsilon^2 \partial_1 v_3), \quad \omega_{ii} = 0, \quad \omega_{13} = \frac{1}{2} (\partial_3 v_1 - \varepsilon^2 \partial_1 v_3) = -\omega_{31}, \\
N_i &= \varepsilon \partial_t n_i + \varepsilon v_i \partial_1 n_i + \varepsilon v_3 \partial_3 n_i - \varepsilon_j^2 \frac{1}{2} \partial_j v_i n_j + \varepsilon_i^2 \frac{1}{2} \partial_i v_j n_j.
\end{aligned}$$

At the substrate $x_3 = 0$, the non-dimensional boundary conditions are

$$v_1 = 0, \quad v_3 = 0, \quad n_3 = \cos \theta_1, \quad q = q_1,$$

and at the free surface, $x_3 = \eta(x_1, t)$, they are

$$\begin{aligned}
\eta_t &= v_3 - v_1 \partial_1 \eta, \\
-p + \frac{\varepsilon}{(1 + \varepsilon^2 \eta_{1,1}^2)} [(\varepsilon^2 T_{11}^E + \tilde{T}_{11}) \eta_{1,1}^2 - (\varepsilon T_{13}^E + \tilde{T}_{13}) \eta_{1,1} - (\varepsilon T_{31}^E + \tilde{T}_{31}) \eta_{1,1} \\
&+ (T_{33}^E + \tilde{T}_{33})] = \frac{\eta_{,11}}{(1 + \varepsilon^2 \eta_{1,1}^2)^{3/2}}, \\
-\varepsilon \eta_{1,1} (\varepsilon^2 T_{11}^E + \tilde{T}_{11}) - \varepsilon^2 \eta_{1,1}^2 (\varepsilon T_{13}^E + \tilde{T}_{13}) + (\varepsilon T_{31}^E + \tilde{T}_{31}) + \varepsilon \eta_{1,1} (T_{33}^E + \tilde{T}_{33}) &= 0, \\
\frac{-\varepsilon \eta_{1,1} n_1 + n_3}{(1 + \varepsilon^2 \eta_{1,1}^2)^{1/2}} &= \cos \theta_2, \quad q = q_2.
\end{aligned}$$

Appendix B. Derivation of the active thin-film Eriksen–Leslie–Parodi model

In this appendix, we give a brief account of the derivation of the thin-film model for the Eriksen–Leslie–Parodi theory augmented by activity terms. Conventions and notations carry over from the main text. The conservation of mass, linear and angular momentum balance equations are

given by

$$0 = \partial_i v_i, \quad (\text{B 1})$$

$$0 = -\partial_i p - \partial_j (\partial_{\partial_j n_k} W \partial_j n_k) + \partial_j \tilde{T}_{ij} \quad (\text{B 2})$$

and

$$0 = h_i - \gamma_1 N_i - \gamma_2 e_{ij} n_j + \lambda_1^* \Delta \chi^* n_i, \quad (\text{B 3})$$

As in the nematic system (2.4)–(2.6), we introduce two active terms with parameters λ_1^* and ζ^* , seen above and, for the latter, in the definition of the extra stress tensor \tilde{T} further below. The bulk free energy density W is given by

$$2W = K_1 (\nabla \cdot \mathbf{n})^2 + K_2 (\mathbf{n} \cdot \text{curl } \mathbf{n})^2 + K_3 (\mathbf{n} \times \text{curl } \mathbf{n})^2 + (K_2 + K_4) (\text{tr}(\nabla n))^2 - (\nabla \cdot \mathbf{n})^2.$$

The parameters K_1 , K_2 and K_3 are the splay, twist and bend elastic moduli [64], and $K_2 + K_4$ is the saddle-splay constant. Note that in the case of strong anchoring, the final term does not contribute to the governing equations [17], and that in two dimensions, there is also no twist term. Again, we will assume that all the $K_1 = K_2 = K_3 \equiv K$ and $K_4 = 0$. This assumption is discussed for liquid crystals in section 3.1.3.2 of [64]), and we use it here for simplification. Note that under this assumption the elastic energy is reduced to the Dirichlet energy $2W = K |\partial_k n_i|^2$ (see also eqn (4) in [17]). The rate of change of the director with respect to the background fluid N_i is defined as in (2.22). The molecular field is given by

$$h_i = \gamma n_i - \frac{\delta W}{\delta n_i}, \quad (\text{B 4})$$

where γ appears as a Lagrange multiplier in the variational formulation to satisfy the condition $n_i n_i = 1$ and may in general depend on x_i and t . The total stress tensor, the Eriksen–Leslie tensor and the extra stress are given by, respectively,

$$\begin{aligned} T_{ij} &= -p \delta_{ij} + T_{ij}^E + \tilde{T}_{ij}, \quad T_{ij}^E = -\partial_{\partial_j n_k} W \partial_j n_k, \\ \tilde{T}_{ij} &= \alpha_1 n_k n_p e_{kp} n_i n_j + \alpha_2 N_i n_j + \alpha_3 N_j n_i + \alpha_4 e_{ij} + \alpha_5 e_{ik} n_k n_j \\ &\quad + \alpha_6 e_{jk} n_k n_i + \zeta^* \Delta \chi^* n_i n_j. \end{aligned}$$

We remark that in some of the literature (e.g. [34]) T_{ij} includes an additional term $-W \delta_{ij}$, which, however, amounts to a redefinition of the pressure [17]. The strong anchoring conditions at the substrate $x_3 = 0$ and the free interface $x_3 = \eta(x, t)$ read

$$n = \sin \theta_1 e_1 + \cos \theta_1 e_3 \quad \text{and} \quad n = \cos \theta_2 v + \sin \theta_2 t,$$

respectively, where e_1 and e_3 are the canonical unit vectors. For the boundary conditions of the flow field, we impose no-slip and impermeability at the substrate (first line), and the kinematic and stress boundary conditions at the interface (second line),

$$\begin{aligned} v_1 &= 0, \quad v_3 = 0, \\ \partial_t \eta &= v_3 - v_1 \partial_1 \eta, \quad v_i T_{ij} = -g_0 \partial_i v_j. \end{aligned}$$

To derive the thin-film approximation, we use the same ansatz for the scalings as before in (3.1), and in addition let $W = \mathcal{E} \bar{W}$, where $\mathcal{E} = K/(\varepsilon^2 L^2)$. We also introduce the dimensionless parameters

$$\bar{\alpha}_i = \frac{\alpha_i}{\mu}, \quad \bar{\gamma}_i = \frac{\gamma_i}{\mu}, \quad \Delta \bar{\chi}^* = \frac{\varepsilon L}{\mu U} \Delta \chi^*, \quad \bar{\zeta}^* = \frac{\zeta^*}{\mu}, \quad \bar{\lambda}_1^* = \lambda_1^*,$$

where μ is the kinematic viscosity. The non-dimensional bulk free energy and the components of the molecular field ($i = 1, 3$) become

$$2\bar{W} = (\partial_3 n_3)^2 + (\partial_3 n_1)^2 + O(\varepsilon^2), \quad \bar{h}_i = n_i + \partial_3^2 n_i + O(\varepsilon^2).$$

For (B 3), we obtain to leading order

$$\frac{K}{\varepsilon \mu U L} \bar{h}_1 - \bar{\alpha}_2 n_3 \partial_3 \bar{v}_1 + \bar{\lambda}_1^* \Delta \bar{\chi}^* n_1 = 0, \quad \frac{K}{\varepsilon \mu U L} \bar{h}_3 - \bar{\alpha}_3 n_1 \partial_3 \bar{v}_1 + \bar{\lambda}_1^* \Delta \bar{\chi}^* n_3 = 0.$$

If $K/\varepsilon\mu UL \gg 1$, the flow field decouples from the director field in these equations, we therefore require weak elasticity $K/\varepsilon\mu UL = O(1)$ and keep all terms in the preceding pair of equations.

The scale P for the pressure is obtained, as before, by balancing it with the dominant viscous contributions in the horizontal momentum equation (B 2) (that is, for $i = 1$). We drop the overbars from this point onwards and introduce θ as before. The leading-order bulk equations then are

$$\begin{aligned} 0 &= v_{1,1} + v_{3,3}, \\ 0 &= -p_{,1} + \frac{1}{2}(v_{1,3}f_A(\theta))_{,3} + \zeta^* \Delta \chi^* (\sin(2\theta))_{,3}, \quad 0 = -p_{,3}, \\ 0 &= \gamma \sin \theta + K(\sin \theta)_{,33} + \frac{1}{2}(\gamma_1 - \gamma_2)v_{1,3} \cos \theta + \lambda_1^* \Delta \chi^* \sin \theta, \\ 0 &= \gamma \cos \theta + K(\cos \theta)_{,33} - \frac{1}{2}(\gamma_1 + \gamma_2)v_{1,3} \sin \theta + \lambda_1^* \Delta \chi^* \cos \theta, \end{aligned}$$

with the Lagrange parameter γ and

$$f_A(\theta) = \left(\frac{\alpha_1}{2}\right) \sin^2(2\theta) + (\alpha_5 - \alpha_2) \cos^2 \theta + (\alpha_3 + \alpha_6) \sin^2 \theta + \alpha_4.$$

Note that in the equations above all terms in $\partial_j(\partial_{\partial_j n_k} W \partial_1 n_k)$ are of order ε or smaller and hence do not contribute. At $x_3 = 0$ (first line) and at $x_3 = \eta(x_1, t)$ (second line) we have, to leading order,

$$\begin{aligned} v_1 &= 0, \quad v_3 = 0, \quad \theta = \theta_1, \\ -p &= \eta_{,11}, \quad v_{1,3}f_B(\theta_2) = -\zeta^* \Delta \chi^* \sin(2\theta_2), \quad \eta_t = v_3 - v_1 \partial_1 \eta, \quad \theta = \theta_2, \end{aligned}$$

with

$$f_B(\theta) = \left(\frac{\alpha_1}{2}\right) \sin^2(2\theta) + (\alpha_6 - \alpha_3) \cos^2 \theta + (\alpha_2 + \alpha_5) \sin^2 \theta + \alpha_4.$$

Similarly as it was done in [17] for its passive counterpart, this system can be integrated to yield the active thin-film model (3.22) based on the Leslie–Erickson–Parodi theory. We note that the director equation (3.22c) automatically implies relation $|n| = \sin^2 \theta + \cos^2 \theta = 1$ and, therefore, Lagrange multiplier γ does not appear in the reduced model (3.22). Also the activity parameter λ_1^* does not enter model (3.22), which is consistent with the absence of the activity parameter in θ -equation (3.21c) of the extended model (3.21), see also relations (3.24).

References

1. Simha RA, Ramaswamy S. 2002 Hydrodynamic fluctuations and instabilities in ordered suspensions of self-propelled particles. *Phys. Rev. Lett.* **89**, 058101. (doi:10.1103/PhysRevLett.89.058101)
2. Kruse K, Joanny JF, Jülicher F, Prost J, Sekimoto K. 2004 Asters, vortices, and rotating spirals in active gels of polar filaments. *Phys. Rev. Lett.* **92**, 078101. (doi:10.1103/PhysRevLett.92.078101)
3. Marchetti MC, Joanny JF, Ramaswamy S, Liverpool TB, Prost J, Rao M, Simha RA. 2013 Hydrodynamics of soft active matter. *Rev. Mod. Phys.* **85**, 1143–1189. (doi:10.1103/RevModPhys.85.1143)
4. Leslie FM. 1968 Some constitutive equations for liquid crystals. *Arch. Ration. Mech. Anal.* **28**, 265–283. (doi:10.1007/BF00251810)
5. Leslie FM. 1979 Theory of flow phenomena in liquid crystals. *Adv. Liquid Cryst.* **4**, 1–81. (doi:10.1016/B978-0-12-025004-2.50008-9)
6. Ericksen JL. 1962 Hydrostatic theory of liquid crystals. *Arch. Ration. Mech. Anal.* **9**, 371–378. (doi:10.1007/BF00253358)
7. Kruse K, Joanny JF, Jülicher F, Prost J, Sekimoto K. 2005 Generic theory of active polar gels: a paradigm for cytoskeletal dynamics. *Eur. Phys. J. E* **16**, 5–16. (doi:10.1140/epje/e2005-00002-5)
8. Jülicher F, Kruse K, Prost J, Joanny JF. 2007 Active behavior of the cytoskeleton. *Phys. Rep.* **449**, 3–28. (doi:10.1016/j.physrep.2007.02.018)
9. Voituriez R, Joanny JF, Prost J. 2006 Generic phase diagram of active polar films. *Phys. Rev. Lett.* **96**, 028102. (doi:10.1103/PhysRevLett.96.028102)

10. Nédélec FJ, Surrey T, Maggs AC, Leibler S. 1997 Self-organization of microtubules and motors. *Nature* **389**, 305–308. (doi:10.1038/38532)
11. Backouche F, Haviv L, Groswasser D, Bernheim-Groswasser A. 2006 Active gels: dynamics of patterning and self-organization. *Phys. Biol.* **3**, 264–273. (doi:10.1088/1478-3975/3/4/004)
12. Voituriez R, Joanny JF, Prost J. 2005 Spontaneous flow transition in active polar gels. *Europhys. Lett.* **70**, 404–410. (doi:10.1209/epl/i2004-10501-2)
13. Sankararaman S, Ramaswamy S. 2009 Instabilities and waves in thin films of living fluids. *Phys. Rev. Lett.* **102**, 118107. (doi:10.1103/PhysRevLett.102.118107)
14. Ben Amar M, Cummings LJ. 2001 Fingering instabilities in driven thin nematic films. *Phys. Fluids* **13**, 1160–1166. (doi:10.1063/1.1359748)
15. Cummings LJ. 2004 Evolution of a thin film of nematic liquid crystal with anisotropic surface energy. *Eur. J. Appl. Math.* **15**, 651–677. (doi:10.1017/S095679250400573X)
16. Cummings LJ, Lin TS, Kondic L. 2011 Modeling and simulations of the spreading and destabilization of nematic droplets. *Phys. Fluids* **23**, 043102. (doi:10.1063/1.3570863)
17. Lin TS, Cummings LJ, Archer AJ, Kondic L, Thiele U. 2013a Note on the hydrodynamic description of thin nematic films: strong anchoring model. *Phys. Fluids* **25**, 082102. (doi:10.1063/1.4816508)
18. Lin TS, Kondic L, Thiele U, Cummings LJ. 2013b Modelling spreading dynamics of nematic liquid crystals in three spatial dimensions. *J. Fluid Mech.* **729**, 214–230. (doi:10.1017/jfm.2013.297)
19. Manyuhina OV, Cazabat AM, Amar MB. 2010 Instability patterns in ultrathin nematic films: comparison between theory and experiment. *Europhys. Lett.* **92**, 16005. (doi:10.1209/0295-5075/92/16005)
20. Manyuhina OV, Ben Amar M. 2013 Thin nematic films: anchoring effects and stripe instability revisited. *Phys. Lett. A* **377**, 1003–1011. (doi:10.1016/j.physleta.2013.01.047)
21. Lam MA, Cummings LJ, Lin TS, Kondic L. 2015 Modeling flow of nematic liquid crystal down an incline. *J. Eng. Math.* **94**, 97–113. (doi:10.1007/s10665-014-9697-2)
22. Beris AN, Edwards BJ. 1994 *Thermodynamics of flowing systems with internal microstructure*, vol. 36. Oxford, UK: Oxford University Press.
23. Zarnescu A. 2012 6. In *Topics in the Q-tensor theory of liquid crystals*, pp. 187–252. Prague: Jindřich Nečas Center for Mathematical Modeling, Lecture Notes Series ‘Topics in Mathematical Modeling and Analysis’, no. 7. Prague, Czech Republic: Matfyzpress.
24. Marenduzzo D, Orlandini E, Yeomans JM. 2007 Hydrodynamics and rheology of active liquid crystals: a numerical investigation. *Phys. Rev. Lett.* **98**, 118102. (doi:10.1103/PhysRevLett.98.118102)
25. Marenduzzo D, Orlandini E, Cates ME, Yeomans JM. 2007b Steady-state hydrodynamic instabilities of active liquid crystals: hybrid lattice Boltzmann simulations. *Phys. Rev. E* **76**, 031921. (doi:10.1103/PhysRevE.76.031921)
26. Rosso R, Virga EG, Kralj S. 2012 Parallel transport and defects on nematic shells. *Continuum Mech. Thermodyn.* **24**, 643–664. (doi:10.1007/s00161-012-0259-4)
27. Zhang R, Zhou Y, Rahimi M, de Pablo JJ. 2016 Dynamic structure of active nematic shells. *Nat. Commun.* **7**, 11773. (doi:10.1038/ncomms11773)
28. Giomi L, Mahadevan L, Chakraborty B, Hagan MF. 2012 Banding, excitability and chaos in active nematic suspensions. *Nonlinearity* **25**, 2245. (doi:10.1088/0951-7715/25/8/2245)
29. Giomi L, Bowick MJ, Mishra P, Sknepnek R, Marchetti MC. 2014 Defect dynamics in active nematics. *Phil. Trans. R. Soc. A* **372**, 20130365. (doi:10.1098/rsta.2013.0365)
30. Thampi SP, Golestanian R, Yeomans JM. 2014 Instabilities and topological defects in active nematics. *Europhys. Lett.* **105**, 18001. (doi:10.1209/0295-5075/105/18001)
31. Marbach S, Godeau AL, Riveline D, Joanny JF, Prost J. 2015 Theoretical study of actin layers attachment and separation. *Eur. Phys. J. E* **38**, 122. (doi:10.1140/epje/i2015-15122-4)
32. Thampi SP, Yeomans JM. 2016 Active turbulence in active nematics. *Eur. Phys. J. Spec. Top.* **225**, 651–662. (doi:10.1140/epjst/e2015-50324-3)
33. Bonelli F, Gonnella G, Tiribocchi A, Marenduzzo D. 2016 Spontaneous flow in polar active fluids: the effect of a phenomenological self-propulsion-like term. *Eur. Phys. J. E* **39**, 1. (doi:10.1140/epje/i2016-16001-2)
34. Rey AD. 2000 Young-Laplace equation for the liquid crystal interfaces. *J. Chem. Phys.* **113**, 10 820–10 822. (doi:10.1063/1.1324993)
35. Rey AD. 1999 Nemato-capillarity theory and the orientation-induced Marangoni flow. *Liq. Cryst.* **26**, 913–917. (doi:10.1080/026782999204606)

36. Rey AD. 2007 Capillarity models for liquid crystal fibers, membranes, films, and drops. *Soft Matter* **3**, 1349–1368. (doi:10.1039/b704248p)
37. Craster RV, Matar OK. 2009 Dynamics and stability of thin liquid films. *Rev. Mod. Phys.* **81**, 1131–1198. (doi:10.1103/RevModPhys.81.1131)
38. Ericksen JL. 1990 Liquid crystals with variable degree of orientation. *Arch. Ration. Mech. Anal.* **113**, 97–120. (doi:10.1007/BF00380413)
39. Sanchez T, Chen DTN, Decamp SJ, Heymann M, Dogic Z. 2012 Spontaneous motion in hierarchically assembled active matter. *Nature* **491**, 431–434. (doi:10.1038/nature11591)
40. Batista VMO, Blow ML, Gama MMTd. 2015 The effect of anchoring on the nematic flow in channels. *Soft Matter* **11**, 4674–4685. (doi:10.1039/C5SM00249D)
41. Carou JQ, Duffy BR, Mottram NJ, Wilson SK. 2015 Steady flow of a nematic liquid crystal in a slowly varying channel. *Mol. Cryst. Liq. Cryst.* **438**, 237–249. (doi:10.1080/15421400590955569)
42. Majumdar A, Zarnescu A. 2010 Landau–de Gennes theory of nematic liquid crystals: the Oseen–Frank limit and beyond. *Arch. Ration. Mech. Anal.* **196**, 227–280. (doi:10.1007/s00205-009-0249-2)
43. Denniston C, Orlandini E, Yeomans JM. 2001 Lattice Boltzmann simulations of liquid crystal hydrodynamics. *Phys. Rev. E* **63**, 056702. (doi:10.1103/PhysRevE.63.056702)
44. Iyer G, Xu X, Zarnescu A. 2015 Dynamic cubic instability in a 2D Q-tensor model for liquid crystals. *Math. Models Methods Appl. Sci.* **25**, 1477–1517. (doi:10.1142/S0218202515500396)
45. Paicu M, Zarnescu A. 2011 Global existence and regularity for the full coupled Navier–Stokes and Q-tensor system. *SIAM J. Math. Anal.* **43**, 2009–2049. (doi:10.1137/10079224X)
46. Majumdar A, Lewis AH. 2017 *A theoretician’s approach to nematic liquid crystals and their applications*, pp. 223–254. Singapore: Springer.
47. Ball JM. 2017 Liquid crystals and their defects. In *Mathematical thermodynamics of complex fluids*. Lecture Notes in Mathematics, pp. 1–46. Cham, Switzerland: Springer.
48. Rey AD. 1999 Marangoni flow in liquid crystal interfaces. *J. Chem. Phys.* **110**, 9769–9770. (doi:10.1063/1.478943)
49. Kitavtsev G, Robbins J, Slastikov V, Zarnescu A. 2016 Liquid crystal defects in the Landau–de Gennes theory in two dimensions—Beyond the one-constant approximation. *Math. Models Methods Appl. Sci.* **26**, 2769–2808. (doi:10.1142/S0218202516500664)
50. Liverpool TB, Marchetti MC. 2005 Bridging the microscopic and the hydrodynamic in active filament solutions. *Europhys. Lett.* **69**, 846–852. (doi:10.1209/epl/i2004-10414-0)
51. Liverpool TB, Marchetti MC. 2004 Comment on “Instabilities of isotropic solutions of active polar filaments”—Reply. *Phys. Rev. Lett.* **93**, 159802. (doi:10.1103/PhysRevLett.93.159802)
52. Liverpool TB, Marchetti MC. 2003 Instabilities of isotropic solutions of active polar filaments. *Phys. Rev. Lett.* **90**, 138102. (doi:10.1103/PhysRevLett.90.138102)
53. Thoumine O, Ott A. 1997 Time scale dependent viscoelastic and contractile regimes in fibroblasts probed by microplate manipulation. *J. Cell Sci.* **110**, 2109–2116.
54. Uhde J, Keller M, Sackmann E, Parmeggiani A, Frey E. 2004 Internal motility in stiffening actin-myosin networks. *Phys. Rev. Lett.* **93**, 268101. (doi:10.1103/PhysRevLett.93.268101)
55. Hatwalne Y, Ramaswamy S, Rao M, Simha RA. 2004 Rheology of active-particle suspensions. *Phys. Rev. Lett.* **92**, 118101. (doi:10.1103/PhysRevLett.92.118101)
56. Mottram NJ, Newton CJP. 2014 Introduction to Q-tensor theory. (<http://arxiv.org/abs/1409.3542>)
57. Teixeira PIC, Sluckin TJ, Sullivan DE. 1993 Landau–de Gennes theory of anchoring transitions at a nematic liquid crystal-substrate interface. *Liq. Cryst.* **14**, 1243–1253. (doi:10.1080/02678299308027834)
58. Ryschenkow G, Kleman M. 1976 Surface defects and structural transitions in very low anchoring energy nematic thin films. *J. Chem. Phys.* **64**, 404–412. (doi:10.1063/1.431934)
59. Whitesides GM. 2006 The origins and the future of microfluidics. *Nature* **442**, 368–373. (doi:10.1038/nature05058)
60. Lavrentovich OD, Pergamenschchik VM. 1995 Patterns in thin liquid crystal films and divergence elasticity. *Int. J. Mod. Phys. B* **9**, 2389–2437. (doi:10.1142/S0217979295000926)
61. Fratta GD, Robbins J, Slastikov V, Zarnescu A. 2016 Half-integer point defects in the Q-tensor theory of nematic liquid crystals. *J. Nonlinear Sci.* **26**, 121–140. (doi:10.1007/s00332-015-9271-8)
62. Khoromskaia D, Alexander GP. 2015 Motility of active fluid drops on surfaces. *Phys. Rev. E* **92**, 062311. (doi:10.1103/PhysRevE.92.062311)
63. Joanny JF, Ramaswamy S. 2012 A drop of active matter. *J. Fluid Mech.* **705**, 46–57. (doi:10.1017/jfm.2012.131)
64. de Gennes PG, Prost J. 1993 *The physics of liquid crystals*. Oxford, UK: Clarendon Press.